LIPID METABOLISM

A bacterial light response reveals an orphan desaturase for human plasmalogen synthesis

Aránzazu Gallego-García[1]*, Antonio J. Monera-Girona[1]*, Elena Pajares-Martínez[1]*, Eva Bastida-Martínez[1], Ricardo Pérez-Castaño[1], Antonio A. Iniesta[1], Marta Fontes[1], S. Padmanabhan[2]†, Montserrat Elías-Arnanz[1]†

Plasmalogens are glycerophospholipids with a hallmark *sn*-1 vinyl ether bond. These lipids are found in animals and some bacteria and have proposed membrane organization, signaling, and antioxidant roles. We discovered the plasmanylethanolamine desaturase activity that is essential for vinyl ether bond formation in a bacterial enzyme, CarF, which is a homolog of the human enzyme TMEM189. CarF mediates light-induced carotenogenesis in *Myxococcus xanthus*, and plasmalogens participate in sensing photooxidative stress through singlet oxygen. TMEM189 and other animal homologs could functionally replace CarF in *M. xanthus*, and knockout of TMEM189 in a human cell line eliminated plasmalogens. Discovery of the human plasmanylethanolamine desaturase will spur further study of plasmalogen biogenesis, functions, and roles in disease.

Plasmalogens are glycerophospholipids with a hydrocarbon chain linked by a vinyl ether bond at the glycerol *sn*-1 position (fig. S1, A and B) found in animals and some anaerobic bacteria but not in plants, fungi, or most aerobic bacteria, except myxobacteria (*1*–*3*). In mammals, plasmalogens are most abundant in the brain, heart, and leukocytes and occur in nearly all subcellular membranes (*1*–*3*). Lipid rafts—membrane microdomain platforms proposed to recruit and activate signaling proteins (*4*)—are enriched in plasmalogens (*5*, *6*). The plasmalogen vinyl ether bond confers physical-chemical attributes that affect membrane fluidity, signaling, and function (*1*, *2*) and is susceptible to cleavage by reactive oxygen species (ROS) such as singlet oxygen ($^1O_2$), yielding products that may act as second messengers (*7*–*10*). Antioxidative and signaling mechanisms have thus been linked to plasmalogens, whose deficiency correlates with various human disorders, including cancer and Alzheimer's disease (*1*, *2*, *11*). Mammalian plasmalogen biosynthesis involves several steps (fig. S2A) (*12*). A key late step in the endoplasmic reticulum (ER) converts an alkyl ether phosphatidylethanolamine (AEPE) or plasmanylethanolamine to the vinyl ether (alkenyl) phosphatidylethanolamine (VEPE) or plasmenylethanolamine (fig. S2A). This oxygen-dependent step was described almost 50 years ago (*13*), but the plasmanylethanolamine desaturase involved is unidentified: an orphan enzyme (*14*, *15*). In the obligately aerobic *Myxococcus xanthus* and related myxobacteria, ether lipid synthesis requires the multifunctional enzyme ElbD and, in an alternative minor pathway, MXAN_1676 (fig. S2B) (*3*, *16*, *17*). ElbD was speculated to also direct vinyl ether bond formation (*16*), but we have discovered that this desaturase activity corresponds to another protein, CarF, and that it is functionally conserved in animals, including humans.

In *M. xanthus*, CarF indirectly signals the light response triggered by $^1O_2$ produced upon photoexcitation of protoporphyrin IX (PPIX) to inactivate a membrane-associated anti-σ factor, CarR, and release its cognate σ factor, CarQ (*18*–*21*). This enables transcription of genes for the biosynthesis of carotenoids, which quench $^1O_2$ and other ROS, and provokes a yellow-to-red color change (the Car^+ phenotype). In another pathway, light directly inactivates a B_{12}-based photoreceptor that represses genes for carotenogenesis in the dark (*22*–*24*). CarF sequence homologs exist in myxobacteria and few other bacteria (mostly Leptospiraceae and Alphaproteobacteria); in invertebrate and vertebrate animal species, including humans, in which they are denoted TMEM189 or Kua and have unknown functions (*19*–*21*, *25*); and in plants, with *Arabidopsis thaliana* having three (At1, At2, and At3) (fig. S3 and table S1). From phylogenetic analyses, myxobacterial and *Leptospira* CarF homologs appear more related to those in animals, and those from Alphaproteobacteria appear more related to ones in plants (fig. S3A). CarF has 12 histidines, all of which are cytoplasmic on the basis of its experimentally determined four-transmembrane helix topology (Fig. 1A), with five shown to be important for function thus far (*19*, *20*). Animal CarF homologs conserve 11 of these histidines, plants conserve eight, and bacteria conserve eight or more (fig. S3 and table S1). To assess the functional importance of each His in vivo, we conditionally expressed, using a vanillate-inducible system, single His-to-Ala N-terminal FLAG-tagged CarF variants in the Car^- *carF*-deleted (Δ*carF*) *M. xanthus* strain. FLAG-tagged CarF is functional because cells that express it were Car^+, as were variants H183A and H190A (in which histidine at positions 183 and 190 was replaced by alanine) and that mutated in the nonconserved His^{218}, whereas the remaining nine His mutants were all Car^- (Fig. 1B). Nine histidines are therefore important in CarF function. All nine are conserved in CarF homologs from other myxobacteria, Leptospirales, and animals, but one of these, His^{113}, differs in plant (where it is often an Arg) and other bacterial homologs (fig. S3 and table S1). The HxxxH and HxxHH pattern of the functionally crucial His^{164}/His^{168} and His^{191}/His^{194}/His^{195}, respectively, occurs in membrane-associated diiron fatty acid desaturases and hydroxylases of otherwise low overall sequence similarity to CarF (*19*–*21*, *25*). Furthermore, At3 is a chloroplast desaturase (FAD4) that generates an unusual trans double bond in the *sn*-2 acyl carbon chain (fig. S1C) (*26*). We therefore investigated whether *M. xanthus* CarF is a desaturase.

Fatty acid methyl ester (FAME) analysis revealed complete absence of a peak in the Δ*carF* strain (Fig. 2A) that in the wild-type *M. xanthus* corresponds to iso15:0-dimethylacetal [i15:0-DMA, indicative ion mass/charge ratio (m/z) = 75] derived from its plasmalogen, MxVEPE (fig. S4) (*16*, *17*). This i15:0-DMA peak was restored in the Δ*carF* strain that expresses a vanillate-inducible *carF* gene (Fig. 2A), indicating that CarF is essential for the production of MxVEPE. We also examined whether the i15:0-DMA peak reappeared when Δ*carF* cell extracts were incubated with pure CarF. After verifying that CarF with a C-terminal Strep tag is functional in *M. xanthus*, we expressed it in *Escherichia coli* and affinity-purified it from the detergent-solubilized membrane fraction (fig. S5). Purified CarF, which contained two equivalents of iron (supplementary materials, materials and methods), tended to slowly form higher-order oligomers possibly detrimental to activity (fig. S5). Consequently, the Δ*carF* cell extract was incubated with freshly purified CarF under aerobic conditions, followed by FAME analysis. Besides molecular oxygen, the desaturase activity that generates the plasmalogen vinyl ether bond requires reduced nicotinamide adenine dinucleotide phosphate (NADPH) and an electron transport chain involving cytochrome b_5 (*27*), as in aerobic fatty acid desaturation (*28*). Hence, we included NADPH and assumed that the extract contains the other necessary components except CarF. Under these conditions, we detected an i15:0-DMA peak, albeit

[1]Departamento de Genética y Microbiología, Área de Genética (Unidad Asociada al Instituto de Química Física "Rocasolano," Consejo Superior de Investigaciones Científicas), Facultad de Biología, Universidad de Murcia, Murcia 30100, Spain. [2]Instituto de Química Física "Rocasolano," Consejo Superior de Investigaciones Científicas, 28006 Madrid, Spain.
*These authors contributed equally to this work.
†Corresponding author. Email: melias@um.es (M.E.-A.); padhu@iqfr.csic (S.P.)

small (Fig. 2A), lending further support to the inference that MxVEPE formation requires CarF.

Single gene disruptions in *M. xanthus* implicated ElbD and, to a minor level, MXAN_1676 in ether lipid biosynthesis and ElbD in the formation of a neutral alkyl (not vinyl) ether lipid that signals fruiting body development and sporulation and is synthesized only upon starvation (*16*, *17*). Because our data implicated CarF, which is crucial in the response to light, to MxVEPE synthesis, we investigated how in-frame gene deletions of *elbD* (Δ*elbD*), *MXAN_1676* (Δ*1676*), or both affected the light response. Single Δ*elbD*- and Δ*1676*-deletion mutants acquired in the light a reddish color, which appeared somewhat less intense for the Δ*elbD* mutant than for the Δ*1676* mutant or the wild-type strain, whereas the double Δ*elbD*Δ*1676* mutant was Car$^-$, like the Δ*carF* strain (Fig. 2B). Consistent with this, activity in the light of a *lacZ* gene fused to the promoter of the carotenogenic gene cluster (*carB*::*lacZ* reporter) was, relative to the wild type, ~60% less for the Δ*elbD* mutant and ~20% less for the Δ*1676* mutant but at low basal levels (no photoinduction) in the Δ*elbD*Δ*1676* mutant, as in the Δ*carF* strain (Fig. 2B). To correlate these data with ether lipid and MxVEPE contents, and to infer the step in plasmalogen biosynthesis at which CarF acts, we performed FAME analysis of each strain. Both i15:0-DMA and iso15:0-*O*-alkylglycerol bis-trimethylsilyl ether (i15:0-OAG-bisTMS, indicative ion m/z = 205, derived from alkyl ether lipids) (fig. S4) were absent in the Δ*elbD*Δ*1676* strain, but consistent with previous findings using single disruption mutants (*16*), both species were present at low levels in the Δ*elbD* strain and closer to wild-type levels in the Δ*1676* strain (Fig. 2C and fig. S6). By contrast, i15:0-OAG, yet not i15:0-DMA, was observed in the Δ*carF* strain (Fig. 2C). Expressing *elbD* or *MXAN_1676* in trans from an inducible promoter in the Car$^-$ Δ*elbD*Δ*1676* strain caused reappearance of ether lipids and plasmalogens and of reddish colony color in the light (fig. S7), ruling out polar effects from the gene deletions. Consistent with the gas chromatography–mass spectrometry (GC-MS) results, direct assessment by means of liquid chromatography–MS (LC-MS)/MS revealed loss of MxVEPE and MxAEPE in the Δ*elbD*Δ*1676* strains but only of MxVEPE in the Δ*carF* mutant (fig. S8). Thus, whereas ElbD or MXAN_1676 enable biosynthesis of alkyl ether lipids, their conversion to the vinyl ether form requires CarF. In other words, CarF appears to be the ether lipid desaturase in plasmalogen synthesis.

Because CarF is implicated in both *M. xanthus* light-induced carotenogenesis and plasmalogen formation, we asked whether the light response depends directly on plasmalogens by supplying them exogenously to the above mutant strains. We used three commercially available plasmalogens typically found in human cells, with an 18(Plasm) chain at the *sn*-1 position and an 18:1 (HsVEPE1), a 20:4 ω-6 (HsVEPE2), or a 22:6 ω-3 (HsVEPE3) chain at the *sn*-2 ester position (Fig. 3A and fig. S9). These human plasmalogens therefore differ from *M. xanthus* MxVEPE, which has i15 chains at both positions (fig. S1B) (*16*, *17*). Yet, all three rescued the Car$^+$ phenotype when fed to the Δ*carF* and Δ*elbD*Δ*1676* strains, as well as to the triple Δ*carF*Δ*elbD*Δ*1676* mutant strain (Fig. 3B and fig. S9). When fed with HsAEPE1, which is HsVEPE1 but with an *sn*-1 alkyl instead of vinyl ether bond (Fig. 3A), the CarF-containing Δ*elbD*Δ*1676* strain became Car$^+$, whereas both Δ*carF* strains remained Car$^-$ (Fig. 3C). Moreover, FAME analysis detected 18:0-DMA and 18:0-OAG (neither natural to *M. xanthus*) in the HsAEPE1-fed Δ*elbD*Δ*1676* mutant but only 18:0-OAG in the Δ*carF*Δ*elbD*Δ*1676* strain (Fig. 3D). Accordingly, LC-MS/MS detected HsAEPE1 and HsVEPE1 in the double mutant but only HsAEPE1 in the triple mutant (fig. S10). This result confirms HsAEPE1 uptake and its conversion, only if CarF is available, to HsVEPE1. Thus, CarF can produce plasmalogen from the corresponding human alkyl ether lipid, despite the latter having *sn*-1 and *sn*-2 moieties that differ from those in the likely natural precursor in *M. xanthus* (fig. S4).

Various human plasmalogens, distinct from the endogenous one, can mediate signaling in *M. xanthus* light-induced carotenogenesis, and CarF can convert a human alkyl ether lipid to its vinyl ether form. We therefore investigated whether human and other eukaryotic homologs, as well as two bacterial ones (neither from myxobacteria), can functionally replace CarF in the *M. xanthus* light response and plasmalogen biosynthesis. Plasmids for vanillate-inducible expression in *M. xanthus* of codon-optimized N-terminal FLAG-tagged homologs from human, mouse, fly, worm, zebrafish (two), *A. thaliana* (three), the animal pathogen *Leptospira interrogans*, and the alphaproteobacterial plant symbiont *Bradyrhizobium diazoefficiens* were constructed, and each was introduced into the Δ*carF* strain. Among cells transformed with the eukaryotic homologs, those expressing animal homologs (41 to 46% identity, 56 to 59% similarity to CarF) (table S1) were all Car$^+$, like those expressing FLAG-tagged or untagged CarF or its version (CarF$_{247}$) lacking the C-terminal 34-residue segment absent in many homologs (Fig. 3E and figs. S3B and S11A). Cells that express the *A. thaliana* homologs (31 to 33% identity to CarF and which do not conserve the functionally crucial H^{113} of CarF) (fig. S3B and table S1) remained Car$^-$, even though these proteins were present at levels comparable with or greater than those of CarF$_{247}$ or the fly homolog (Fig. 3E).

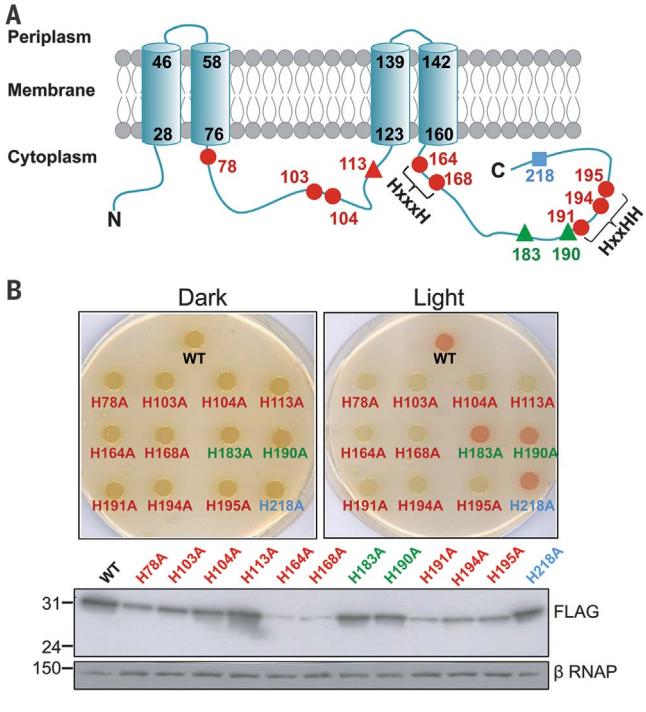

Fig. 1. *M. xanthus* CarF and histidine mutational analysis. (**A**) Experimentally determined membrane topology of CarF (*20*) and location of its 12 histidines. Numbers indicate residues in the CarF sequence. Histidines conserved in all homologs are shown as dots, those conserved only in some homologs are shown as triangles, and both are colored according to their mutation to alanine affects (red) or not (green) CarF function. The blue square is for a nonconserved histidine. (**B**) Mutational analysis of histidines in CarF. Each cell spot corresponds to the *M. xanthus* Δ*carF* strain expressing wild-type (WT) CarF or the indicated His-to-Ala mutant version. Cells that express a nonfunctional CarF variant do not undergo the yellow-to-red color change when exposed to light (supplementary materials, materials and methods). (Bottom) A Western blot of *M. xanthus* cell extracts expressing each CarF variant probed by using anti-FLAG and anti-RNAP β antibodies (as loading control), with sizes (in kilodaltons) indicated on the left.

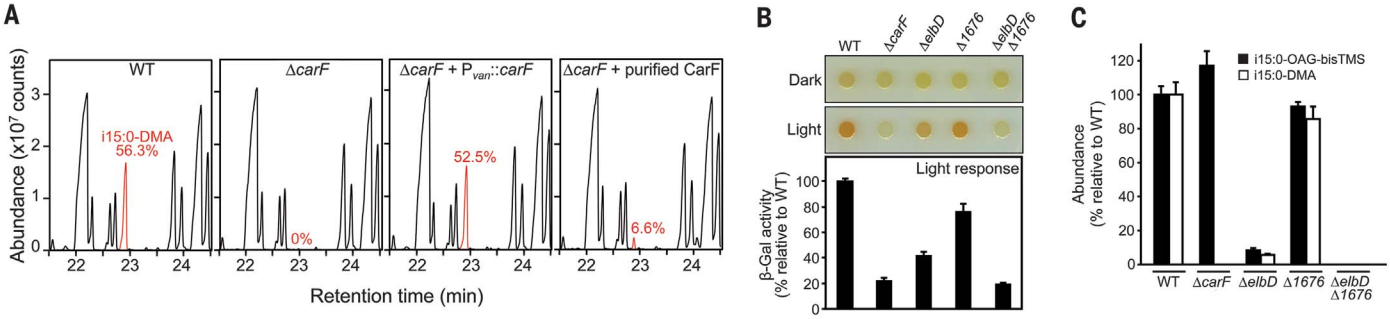

Fig. 2. CarF mediates plasmalogen synthesis in *M. xanthus*. (**A**) FAME GC-MS chromatogram sections of total lipid extracts from *M. xanthus* strains. i15:0-DMA peak level is shown (in percent) relative to fixed amount of 17:0 internal standard. (**B**) Light-induced colony color assay and light-inducible *carB*::*lacZ* reporter probe assay [mean and standard errors, n = 3 biological replicates; WT levels set to 100%]. (**C**) Relative abundance of i15:0-DMA and i15:0-OAG-bisTMS (fig. S4) for indicated *M. xanthus* strains (mean and standard errors, n = 3 biological replicates; normalized to fixed amount of internal 17:0 standard and WT levels set to 100%).

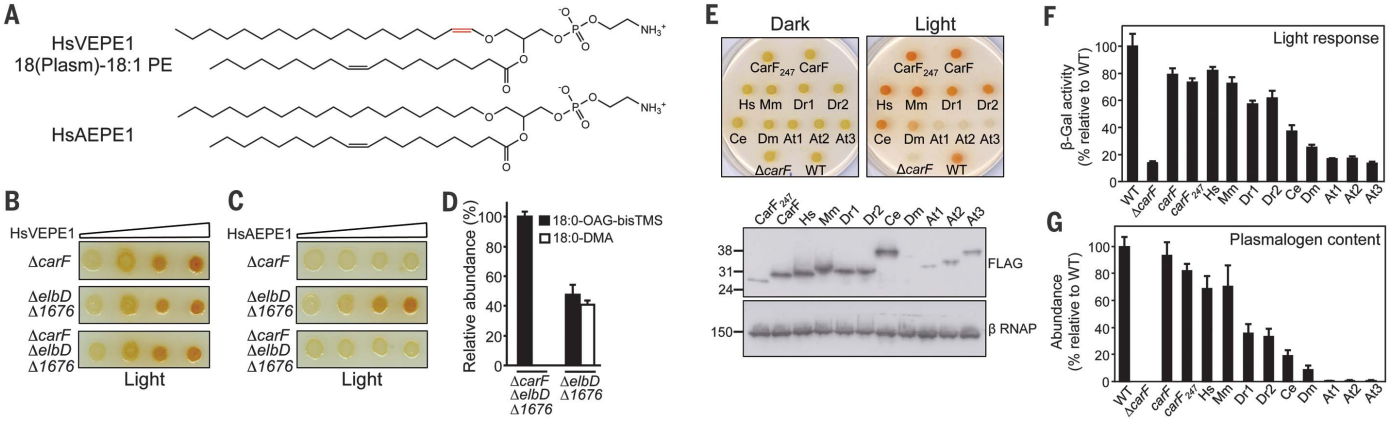

Fig. 3. Plasmalogens mediate signaling of *M. xanthus* light-induced carotenogenesis, and animal but not plant CarF homologs enable plasmalogen synthesis and light-induced carotenogenesis in *M. xanthus*. (**A**) HsVEPE1 and HsAEPE1 chemical structures. (**B** and **C**) Rescue of light-induced carotenogenesis upon feeding *M. xanthus* strains with (B) HsVEPE1 or (C) HsAEPE1. (**D**) Detection of 18:0-OAG-bisTMS and 18:0-DMA in indicated *M. xanthus* strains, with 17:0 as internal standard (mean and standard errors, n = 3 biological replicates, relative to 18:0-OAG-bisTMS set to 100% in the Δ*carF*Δ*elbD*Δ*1676* strain). (**E**) Light-induced colony-color assay with the Δ*carF* strain expressing CarF or CarF$_{247}$ (as controls) and animal (Hs, Mm, Dr1, Dr2, Ce, or Dm) or plant (At1, At2, or At3) CarF homologs, all N-terminally FLAG-tagged. Western blots of the corresponding *M. xanthus* cell extracts are shown below, with sizes (in kilodaltons) indicated on the left. (**F**) Light-inducible *carB*::*lacZ* reporter assay in strains used in (E). (**G**) Abundance of i15:0-DMA relative to internal 17:0 standard in strains used in (E). Values in (F) and (G) are mean and standard errors (n = 3 biological replicates) relative to 100% for the wild type.

Consistently, light-induced *carB*::*lacZ* reporter activity was greater than basal levels in Δ*carF* strains that express animal, but not *A. thaliana*, homologs (Fig. 3F); and in FAME analysis, the i15:0-DMA peak reappeared only in cells that express the animal homologs (Fig. 3G and fig. S11, B and C). Of the two bacterial homologs tested, only the one more related to animal homologs, that from *L. interrogans* (43% identity to CarF), could functionally replace CarF in *M. xanthus* (fig. S12). Thus, animal TMEM189 proteins can use the endogenous *M. xanthus* ether lipid precursor, despite it being different from their natural substrates, to generate MxVEPE.

Given the above results, we further examined human TMEM189. Eleven of the 12 histidines in CarF are conserved in TMEM189 (fig. S3B), and single mutations of nine of these to Ala impaired function in *M. xanthus* (Fig. 4A), just as with the equivalent mutations in CarF (Fig. 1B), thus providing further evidence that the two proteins are closely related. Hence, we tested whether TMEM189 is the plasmanylethanolamine desaturase in human plasmalogen synthesis by using cell lines. We obtained a HAP1 human cell line with a CRISPR/Cas9 *TMEM189* knockout (KO) to compare its ether lipid content with that of the parental cells by means of FAME analysis. Plasmalogens were detected as 16:0-, 18:0-, and 18:1-DMA peaks in the parental cells but were absent in their *TMEM189*-KO derivative, whereas their alkyl ether lipid precursors were detected as the corresponding OAG-bisTMS derivatives in both cell lines (Fig. 4B and fig. S13). Moreover, plasmalogens reappeared in the *TMEM189*-KO cells upon transient expression of EGFP-TMEM189 (fig. S14), and this functional EGFP-fused protein localized in HeLa cells to the ER (Fig. 4C), the proposed site for vinyl ether bond generation in plasmalogen biosynthesis (fig. S2A).

Our study reveals TMEM189 as the long-sought desaturase for animal plasmalogen biosynthesis and that its plant homologs lack this activity. Identification of the animal plasmanylethanolamine desaturase allows direct studies of the nexus between plasmalogens, their cellular functions, and diverse pathologies, which have thus far relied on targeting genes involved earlier in the biosynthetic pathway. We also establish plasmalogens as crucial in the $^1O_2$ response triggered by photoexcitation of PPIX mentioned earlier (*21*). $^1O_2$ is known to provoke cleavage of the plasmalogen at its vinyl ether bond, yielding as breakdown

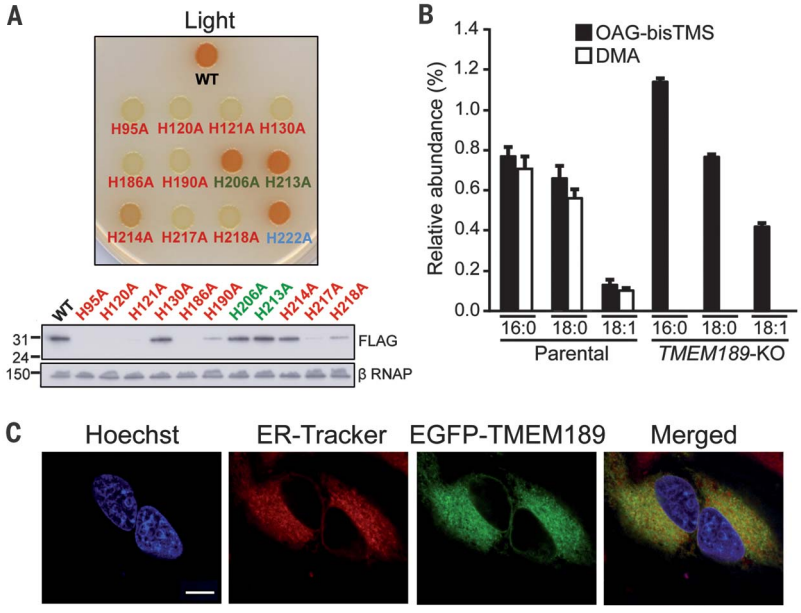

Fig. 4. Analysis of human TMEM189. (**A**) Mutational analysis of histidines in human TMEM189. Each spot corresponds to a Δ*carF M. xanthus* strain expressing, from a vanillate-inducible promoter, TMEM189 (WT), or the indicated His-to-Ala mutant version, all N-terminally FLAG-tagged. Mutation of the nonconserved His^{222} is also shown. Western blots of the corresponding *M. xanthus* cell extracts are shown below, with sizes (in kilodaltons) indicated on the left. (**B**) Levels in the parental and *TMEM189*-KO human HAP1 cells of ether lipids and plasmalogens measured as OAG-bisTMS and DMA, respectively, by means of FAME GC-MS analysis (mean and standard errors relative to total, $n = 3$ biological replicates). (**C**) Localization of human TMEM189 with an N-terminal fusion to enhanced green fluorescent protein in transfected human HeLa cells monitored with confocal microscopy. Scale bar, 10 μm. ER-Tracker and Hoechst 33258 were used to image the ER and nuclear DNA, respectively.

products 2-monoacylglycerophosphoethanolamine (lyso-PE) and a fatty aldehyde (fig. S15) (*7*–*10*). Plasmalogen cleavage by $^1O_2$ to lyso-PE likely perturbs local membrane structure and properties, and adduct formation with the fatty aldehyde can render membrane proteins inactive (*1*, *2*, *7*). Either or both conceivably underlie the light-$^1O_2$-plasmalogen signaling mechanism that leads to CarR inactivation, CarQ release, and induction of carotenogenesis in *M. xanthus* (fig. S16), although a less likely mechanism without plasmalogen breakage cannot be excluded.

REFERENCES AND NOTES

1. N. E. Braverman, A. B. Moser, *Biochim. Biophys. Acta* **1822**, 1442–1452 (2012).
2. J. M. Dean, I. J. Lodhi, *Protein Cell* **9**, 196–206 (2018).
3. H. Goldfine, *FEBS Lett.* **591**, 2714–2719 (2017).
4. E. Sezgin, I. Levental, S. Mayor, C. Eggeling, *Nat. Rev. Mol. Cell Biol.* **18**, 361–374 (2017).
5. L. J. Pike, X. Han, K. N. Chung, R. W. Gross, *Biochemistry* **41**, 2075–2088 (2002).
6. C. Rodemer *et al.*, *Hum. Mol. Genet.* **12**, 1881–1895 (2003).
7. C. M. Jenkins *et al.*, *J. Biol. Chem.* **293**, 8693–8709 (2018).
8. O. H. Morand, R. A. Zoeller, C. R. Raetz, *J. Biol. Chem.* **263**, 11597–11606 (1988).
9. R. A. Zoeller, O. H. Morand, C. R. Raetz, *J. Biol. Chem.* **263**, 11590–11596 (1988).
10. S. Stadelmann-Ingrand, S. Favreliere, B. Fauconneau, G. Mauco, C. Tallineau, *Free Radic. Biol. Med.* **31**, 1263–1271 (2001).
11. M. C. F. Messias, G. C. Mecatti, D. G. Priolli, P. de Oliveira Carvalho, *Lipids Health Dis.* **17**, 41 (2018).
12. N. Nagan, R. A. Zoeller, *Prog. Lipid Res.* **40**, 199–229 (2001).
13. R. L. Wykle, M. L. Blank, B. Malone, F. Snyder, *J. Biol. Chem.* **247**, 5442–5447 (1972).
14. T. Harayama, H. Riezman, *Nat. Rev. Mol. Cell Biol.* **19**, 281–296 (2018).
15. K. Watschinger, E. R. Werner, *Biochimie* **95**, 59–65 (2013).
16. W. Lorenzen, T. Ahrendt, K. A. Bozhüyük, H. B. Bode, *Nat. Chem. Biol.* **10**, 425–427 (2014).
17. M. W. Ring *et al.*, *J. Biol. Chem.* **281**, 36691–36700 (2006).
18. M. Elías-Arnanz, S. Padmanabhan, F. J. Murillo, *Curr. Opin. Microbiol.* **14**, 128–135 (2011).
19. M. Fontes, L. Galbis-Martínez, F. J. Murillo, *Mol. Microbiol.* **47**, 561–571 (2003).
20. L. Galbis-Martínez, M. Galbis-Martínez, F. J. Murillo, M. Fontes, *Microbiology* **154**, 895–904 (2008).
21. M. Galbis-Martínez, S. Padmanabhan, F. J. Murillo, M. Elías-Arnanz, *J. Bacteriol.* **194**, 1427–1436 (2012).
22. M. Jost *et al.*, *Nature* **526**, 536–541 (2015).
23. J. M. Ortiz-Guerrero, M. C. Polanco, F. J. Murillo, S. Padmanabhan, M. Elías-Arnanz, *Proc. Natl. Acad. Sci. U.S.A.* **108**, 7565–7570 (2011).
24. S. Padmanabhan, M. Jost, C. L. Drennan, M. Elías-Arnanz, *Annu. Rev. Biochem.* **86**, 485–514 (2017).
25. T. M. Thomson *et al.*, *Genome Res.* **10**, 1743–1756 (2000).
26. J. Gao *et al.*, *Plant J.* **60**, 832–839 (2009).
27. M. L. Blank, F. Snyder, *Methods Enzymol.* **209**, 390–396 (1992).
28. H. Goldfine, *Prog. Lipid Res.* **49**, 493–498 (2010).

ACKNOWLEDGMENTS

We thank C. L. Drennan (MIT) for critical comments on the manuscript; D. González-Silvera and P. L. Valero for advice on lipid analysis; J. A. Madrid and V. López-Egea for technical assistance; personnel at the instrumentation, sequencing, tissue culture, and confocal microscopy facilities (all at the University of Murcia); and J. Abellón-Ruiz (Newcastle University) for the exchange on membrane protein purification. **Funding:** This work was supported by grants BFU2015-67968-C2-1P and PGC2018-094635-B-C21 (to M.E.-A.) and BFU2015-67968-C2-2P and PGC2018-094635-B-C22 (to S.P.) from the Agencia Estatal de Investigación (AEI)–Spain and the European Regional Development Fund (FEDER), by grants 19429/PI/14 and 20992/PI/18 (to M.E.-A.) from Fundación Séneca (Murcia)-Spain, and Ph.D. fellowship contracts from the Ministerio de Educación y Cultura-Spain (to E.P.-M., A.J.M.-G., and E.B.-M.) and Ministerio de Economía y Competitividad-Spain (to R.P.-C.). **Author contributions:** M.E.-A. conceived the study. M.E.-A., S.P., and A.G.-G. designed experiments, with input from other authors. A.J.M.-G., E.P.-M., A.G.-G., E.B.-M., R.P.-C, M.F., and A.A.I. performed the experiments. All authors contributed to data analysis. A.G.-G., M.F., S.P., and M.E.-A. supervised research. S.P. and M.E.-A. acquired funding, wrote the original draft, and reviewed and edited it with input from all authors. **Competing interests:** The authors declare no competing interests. **Data and materials availability:** All data are available in the main text or the supplementary materials, and strains and plasmids are available upon request.

SUPPLEMENTARY MATERIALS

science.sciencemag.org/content/366/6461/128/suppl/DC1
Materials and Methods
Figs. S1 to S16
Tables S1 to S3
References (*29*–*40*)

29 May 2019; accepted 4 September 2019
10.1126/science.aay1436

Science

A bacterial light response reveals an orphan desaturase for human plasmalogen synthesis

Aránzazu Gallego-García, Antonio J. Monera-Girona, Elena Pajares-Martínez, Eva Bastida-Martínez, Ricardo Pérez-Castaño, Antonio A. Iniesta, Marta Fontes, S. Padmanabhan and Montserrat Elías-Arnanz

Science **366** (6461), 128-132.
DOI: 10.1126/science.aay1436

Distant cousin helps spot animal enzyme

In addition to forming the membranes that enclose cells, lipids are important signaling molecules. Plasmalogens, which contain a vinyl ether linkage, are an abundant group of lipids in animals. How these lipids are synthesized from precursors with an alkyl ether linkage has been a mystery. Gallego-García *et al.* found an enzyme, CarF, in the social bacterium *Myxococcus xanthus* that produces plasmalogens used in a signaling pathway for singlet oxygen, a marker of photooxidative stress. They then showed that the animal homolog could catalyze the final step in plasmalogen synthesis in bacterial and human cells, thus resolving a source for plasmalogens in animals.

Science, this issue p. 128